Dalton Transactions

RSC Publishing

PAPER

View Article Online
View Journal | View Issue

Cite this: *Dalton Trans.*, 2013, **42**, 4081

Sensitivity of [Ru(phen)$_2$dppz]$^{2+}$ light switch emission to ionic strength, temperature, and DNA sequence and conformation†

Andrew W. McKinley,[a] Per Lincoln[b] and Eimer M. Tuite*[c]

Received 24th October 2012,
Accepted 11th January 2013

DOI: 10.1039/c3dt32555e

www.rsc.org/dalton

The luminescence of DNA-bound [Ru(phen)$_2$dppz]$^{2+}$ is shown to be highly sensitive to environmental conditions such as ionic strength, temperature, and the sequence and secondary structure of the nucleic acid, although not to bulky DNA substituents in the major groove. Each enantiomer has two characteristic lifetimes with any polynucleotide and their relative amplitudes vary as a function of binding ratio. For [poly(dA-dT)]$_2$ as a model sequence, the longer lifetime for Δ-[Ru(phen)$_2$dppz]$^{2+}$ has been assigned to canted intercalation of the complex and the shorter lifetime is ascribed to symmetric intercalation. At a fixed binding ratio, the longer lifetime amplitude increases with increasing ionic strength, without significant change in lifetimes. Increasing temperature has a similar effect, but also affects lifetimes. In general, emission is strongest with AT-rich polynucleotides and with higher-order secondary structures, with intensity increasing as single-stranded < duplex < triplex. However, sequence-context and secondary duplex structure also influence the photophysics since emission with [poly(dA)]·[poly(dT)] is significantly higher than with [poly(dA-dT)]$_2$ or [poly(rA)]·[poly(rU)]. The strong influence of different environmental conditions on the emission of nucleic acid-bound [Ru(phen)$_2$dppz]$^{2+}$ reflects subtle heterogeneities that are inherent elements of DNA recognition by small molecules, amplified by large changes in photophysics caused by differential exposure of the dppz nitrogens to groove hydration.

Introduction

[Ru(phen)$_2$dppz]$^{2+}$ (dppz = dipyrido[3,2-*a*:2′,3′-*c*]phenazine; phen = phenanthroline) (Fig. 1) is the archetypal "light-switch" metal complex for recognition of DNA.[1] It is essentially non-luminescent in water but shows remarkably increased emission on binding to DNA[1,2] as well as in organic solvents[3,4] and hydrophobic microenvironments.[5,6] This results from differential population of two close-lying dppz-localized ^{3}MLCT states,[7–11] with the non-emissive state favoured in polar and H-bonding solvents.[12–15] The formation of H-bonds between water and the 9,14-nitrogens on the extended (phenazine) portion of the dppz ring helps to stabilise the dark state which becomes dominant, resulting in non-emissive behaviour in water. Both phenazine nitrogens must be H-bonded to completely extinguish ^{3}MLCT luminescence.[15]

As a general DNA fluorescent probe, [Ru(phen)$_2$dppz]$^{2+}$ suffers the disadvantage of having a sequence-dependent quantum yield.[16–18] The corollary is that it has potential to report on the sequence and structure of nucleic acids. In this respect, the emission of [Ru(phen)$_2$dppz]$^{2+}$ and [Ru(bpy)$_2$dppz]$^{2+}$ with duplex DNAs has been reported for both the racemate[16] and enantiomers.[17,18] Additionally, interactions of [Ru(phen)$_2$dppz]$^{2+}$ and related compounds have been reported with single-stranded,[19–21] triplex,[22] quadruplex and i-motif[21] DNA, and with RNA duplex[16] and triplex.[23]

Finally, the complex has been proposed as a probe for DNA mismatches, since luminescence of [Ru(bpy)$_2$dppz]$^{2+}$ is greater

[a]*Department of Chemistry, Imperial College London, London SW7 2AZ, United Kingdom. E-mail: a.mckinley@imperial.ac.uk*
[b]*Department of Chemical and Biological Engineering, Physical Chemistry, Chalmers University of Technology, SE-41296 Göteborg, Sweden. E-mail: lincoln@chalmers.se; Fax: +46 31 772305; Tel: +46 31 7723055*
[c]*School of Chemistry, Bedson Building, Newcastle University, Newcastle upon Tyne NE1 7RU, United Kingdom. E-mail: eimer.tuite@ncl.ac.uk; Fax: +44 (0) 191 2226929; Tel: +44 (0) 191 2225523*
†Electronic supplementary information (ESI) available: Additional figures and tables. See DOI: 10.1039/c3dt32555e

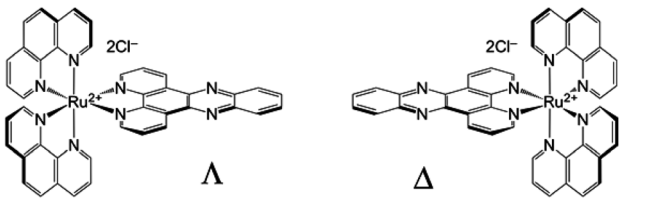

Fig. 1 Structures of the [Ru(phen)$_2$dppz]$^{2+}$ enantiomers.

when metalloinserted at an A–A mismatch than when bound to the consensus duplex.[24,25]

When bound to nucleic acids, the emission decay is multi-exponential. We have previously reported the variation in lifetimes of Δ- and Λ-$[Ru(phen)_2dppz]^{2+}$ bound to different DNA polynucleotides.[17,18] For a single enantiomer with a homopolynucleotide, two discrete lifetimes are observed and their relative amplitudes vary with the $[Ru(phen)_2dppz]^{2+}$/nucleotide ([Ru]/[Nu]) ratio. Lifetimes are generally longer for the Δ-enantiomer and with AT-rich sequences. For either enantiomer with mixed sequences, *e.g.* calf-thymus DNA, both the magnitude of the lifetimes and their relative amplitudes vary with [Ru]/[Nu].[2]

We have recently developed a binding model[26] for Δ-$[Ru(L)_2dppz]^{2+}$ with $[poly(dA\text{-}dT)]_2$ as a model sequence. In our model, the ruthenium centre lies in the minor groove, consistent with room temperature NMR results.[27,28] The model was derived from simultaneous fitting of photophysical and calorimetry data, and assigns the two lifetimes to different intercalation geometries. In one geometry, the dppz ligand is perpendicular to the base pair long axis (*symmetric intercalation*), and in the other it is rotated towards the base pair long axis (*canted intercalation*). Similar geometries were previously proposed by Barton and coworkers[16] for intercalation from the major groove, since the minor groove was considered too narrow to accommodate such binding heterogeneity. However, recent crystal structures have demonstrated differently angled intercalation geometries for intercalation from the minor groove,[29,30] consistent with heterogeneity of intercalation observed in NMR studies.[27] The existence of two modes of binding in a single site, with different thermodynamics, has been recently reported also for the minor groove binder netropsin.[31] No previous model has successfully explained the physical basis for the variation of lifetimes and amplitudes with binding ratio and sequence. In our model, canted intercalation occurs at either end of contiguously intercalated complexes, and symmetric intercalation occurs for "sandwiched" complexes and for isolated binders (Fig. 2).

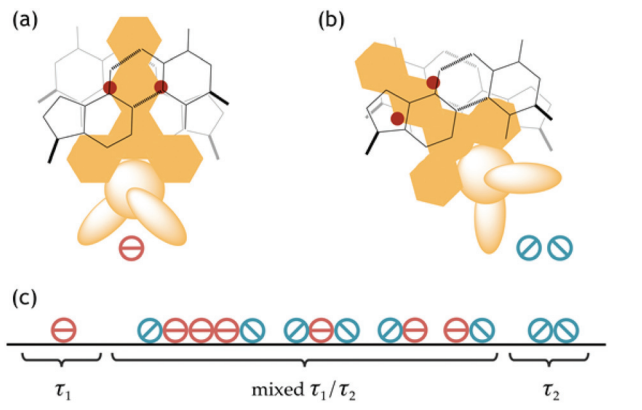

Fig. 2 Cartoon illustrating the orientation of the complex in (a) symmetric (⊖) and (b) canted (⊘) intercalation geometries, and (c) the distributions possible for the two orientations $[Ru(phen)_2dppz]^{2+}$ bound to $[poly(dA\text{-}dT)]_2$.

Partitioning between the two geometries is observed to depend on L (phen or bpy) and [Ru]/[Nu].[26] Analysis of the thermodynamics shows that partitioning is largely dictated by anti-cooperative interactions between the ancillary ligands of adjacently intercalated complexes being offset by cooperative interactions between the ancillary ligand and DNA backbone. These effects are more pronounced for the larger phenanthroline ligand. For Δ-$[Ru(L)_2dppz]^{2+}$ with $[poly(dA\text{-}dT)]_2$, the shorter lifetime is assigned to symmetric intercalation (τ_1), where both phenazine nitrogens are exposed to the major groove.[26] However, for other systems, τ_1 could be either the shorter or longer lifetime, depending on the exposure of the nitrogens in the two geometries.[18]

We previously focused our attention on binding of $[Ru(phen)_2dppz]^{2+}$ and $[Ru(bpy)_2dppz]^{2+}$ to alternating polynucleotides as a function of binding ratio. We reported how the lifetimes and pre-exponential factors for biexponential emission[17,18] as well as the related thermodynamics,[26] depend on enantiomer, ancillary ligand, and sequence. In this paper, we report how the emission of $[Ru(phen)_2dppz]^{2+}$ enantiomers also depends on DNA and RNA primary and secondary structure, as well as variations in ionic strength and temperature. Hence, although this complex has the potential to report on unusual DNA structures, it is necessary to be aware of the many variables which can strongly affect the emission quantum yield of a $[Ru(phen)_2dppz]^{2+}$/nucleic acid sample.

Experimental

Enantiomers of $[Ru(phen)_2dppz]Cl_2$ were prepared and purified as previously described.[2,32] Excitation spectroscopy was used to establish that emissive ruthenium complex impurities contributed <0.1% to the emission. Enantiomeric purity was established by CD spectroscopy (Jasco J-720). The concentration of $[Ru(phen)_2dppz]^{2+}$ in HPLC-grade water was determined using the molar extinction coefficient ε(440 nm) = 20 000 M^{-1} cm^{-1}.[2] Calf thymus (CT), T4, T2, *E. coli*, *M. lysodeikticus* and *C. perfringens* DNA were from Sigma. Synthetic RNA polynucleotides [poly(rA)] and [poly(rA)]·[poly(rU)] and DNA polynucleotides $[poly(dA\text{-}dT)]_2$, $[poly(dG\text{-}dC)]_2$, $[poly(dI\text{-}dC)]_2$, poly(dA-dG)]·[poly(dC-dT)], [poly(dA-dC)]·[poly(dG-dT)], [poly(dA)]·[poly(dT)], [poly(dG)]·[poly(dC)], [poly(dI)]·[poly(dC)], [poly(dA)], [poly(dT)], were from Amersham-Pharmacia (now GE Healthcare). Commercial nucleic acid samples were supplied as lyophilized solids and were dissolved in HPLC-grade water. Solutions were dialysed (EDTA-treated SpectraPor-2 dialysis tubing, Spectrum) extensively against HPLC-grade water, then against 5 mM sodium phosphate buffer (pH 6.9). DNA samples were filtered through 0.45 μm Millipore filters before storage at −20 °C. Nucleic acid concentrations were determined using the extinction coefficients provided by the supplier (ESI;† Table S9); stated concentrations are those of nucleotide repeat units. Triplex [poly(dT)]*[poly(dA)]·[poly(dT)] was prepared by incubating a 1 : 2 molar ratio of poly(dA) and poly(dT) at 90 °C for 30 min followed by 24 h annealing

at room temperature in 5 mM phosphate buffer (pH 6.9) containing 150 μM $MgCl_2$. Formation of triplex was confirmed by its characteristic CD spectrum[33] and melting profile.

Absorption spectra were measured with a Cary 100-Bio UV/vis spectrometer. Emission and excitation spectra were recorded on a SPEX Fluoromax spectrofluorimeter. Emission lifetimes were determined by the frequency modulation method using a SPEX Fluorolog-tau instrument; broadband emission was detected using a high-pass filter for $\lambda > 540$ nm. For several samples, comparable results were obtained by single photon counting with detection at the maximum emission wavelength. Emission measurements were made using 10 × 4 mm or 10 × 2 mm semi-micro emission cuvettes, with excitation along the short path to minimize inner filter effects. No spectral perturbations due to aggregation of complex were observed for complex concentrations below 30 μM at low ionic strength.

Frequency modulation reports the relative fractional luminescence amplitude (f_i) for each lifetime (τ_i), which is converted to relative pre-exponential factor (α_i) by eqn (2):[34]

$$I(t) = I_0[\alpha_1 \exp(-t/\tau_1) + \alpha_2 \exp(-t/\tau_2)] \quad (1)$$

$$\alpha_i = \frac{f_i/\tau_i}{\sum f_i/\tau_i} \quad (2)$$

For a constant total population of excited states, the relative steady-state emission intensity is calculated as the sum of the lifetimes multiplied by their pre-exponential factors:

$$I(\text{calc}) = \Sigma(\alpha_i \times \tau_i) \quad (3)$$

Experiments with polynucleotides were generally performed at low ionic strength in water to maximize electrostatic interactions of the ruthenium complexes with the nucleic acids, and to avoid aggregation of complex that might occur at high ionic strength. The standard buffer was 5 mM sodium phosphate (pH 6.9) in HPLC-grade water. NaCl and $MgCl_2$ used to increase ionic strength were of molecular biology grade (Sigma).

Results

Emission with alternating polynucleotides

Both enantiomers of $[Ru(phen)_2dppz]^{2+}$ exhibit two lifetimes when intercalated with the alternating DNA homopolymer $[poly(dA\text{-}dT)]_2$ and the magnitudes of the double exponential lifetimes depend on enantiomer. Fig. 3 shows a global analysis of single photon counting data for Δ- and Λ-$[Ru(phen)_2dppz]^{2+}$ bound to $[poly(dA\text{-}dT)]_2$. The pattern of pre-exponential factor variation with [Nu]/[Ru] corresponds with our previously reported frequency domain results (ESI;† Tables S1–S4).[18]

We find no measurable effect of argon- or oxygen-saturation on the emission of $[Ru(phen)_2dppz]^{2+}$ bound to DNA, even though O_2 is a good quencher in organic solvents.[4] Thus, the emissive ^{3}MLCT state is well protected from dissolved gases in solvent when the complex is intercalated. The pre-exponential factors vary with binding ratio, with τ_S dominating at high [Nu]/[Ru]. Hence, the emission quantum yield and the measured luminescence intensity vary with [Nu]/[Ru] for each system. The relative enhancements vary with nucleic acid sequence and the nature of the ancillary ligand, as well as enantiomer.[18] In addition, we now report that emission is sensitive to two further experimental conditions, namely temperature and ionic strength.

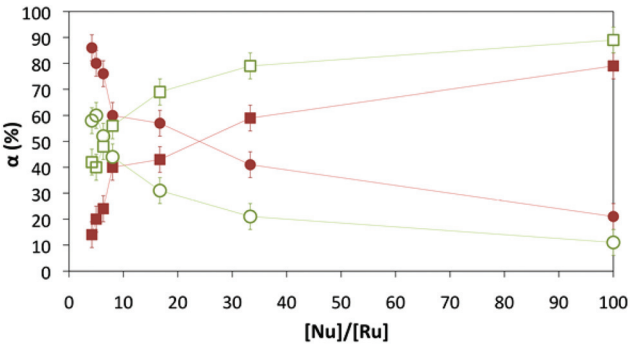

Fig. 3 Pre-exponential factors (α_i) for enantiomers of $[Ru(phen)_2dppz]^{2+}$ bound to $[poly(dA\text{-}dT)]_2$. Δ- = closed symbols; τ_L = 773 (29) ns, ●; τ_S = 132 (9) ns, ■. Λ- = open symbols; τ_L = 297 (5) ns, ○; τ_S = 37 (2) ns, □. λ_{ex} = 337 nm; λ_{em} = 620 nm. [Ru] = 25 μM; 1 mM cacodylate/10 mM NaCl (pH 7) buffer; 25 °C.

Influence of ionic strength on emission

The steady-state emission of Δ-$[Ru(phen)_2dppz]^{2+}$ bound to $[poly(dA\text{-}dT)]_2$ increases with ionic strength (lower panels, Fig. 4 and 5; ESI† Tables S5 and S6); significant changes are observed at [Nu]/[Ru] = 50 with smaller changes at [Nu]/[Ru] = 6. The biexponential lifetimes are essentially invariant as the ionic strength is raised; thus, intensity enhancements result principally from increased population of the long-lived excited state, as evident in Fig. 4 and 5 (upper panels). The two lifetimes are associated with different intercalation geometries for binding from the minor groove, symmetric (τ_S) and canted (τ_L),[18,26] and their relative populations are dictated by a balance of dye–dye and dye–DNA interactions. Altered pre-exponential factors at a fixed binding ratio indicate a shift in equilibrium between binding modes, implying that dye–dye and dye–DNA interactions are differently influenced by ionic strength.

At [Nu]/[Ru] = 50, for ionic strength below 150 mM Na^+ or 10 mM Mg^{2+}, the measured steady state emission intensity coincides with that predicted from time-resolved data. At higher NaCl concentrations, the measured intensity drops below the prediction, indicating displacement of bound dye as expected from the ionic strength dependence of Δ-$[Ru(phen)_2dppz]^{2+}$ binding to CT-DNA ($\delta \log K/\delta[Na^+] \approx 2$).[35]

At [Nu]/[Ru] = 50 in 5 mM phosphate, nearly 80% of the excited states decay with the short lifetime. This drops to ~60% on addition of 150 mM NaCl, and to ~40% with a further increase to 1.2 M NaCl. This behaviour accounts for the higher proportion of long lifetime species observed in our

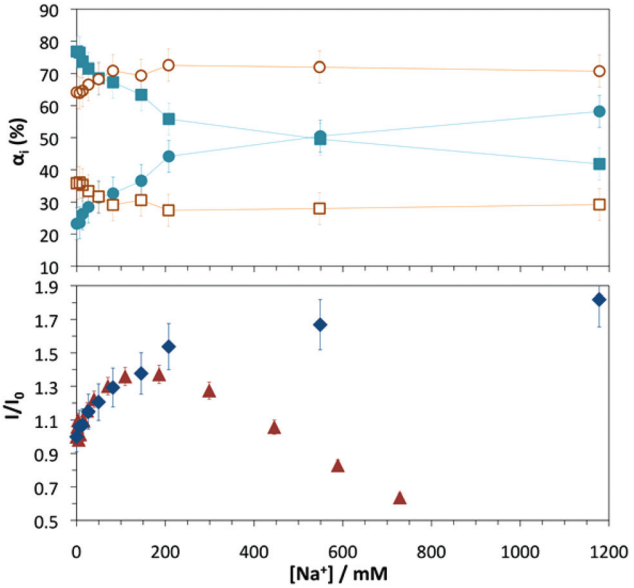

Fig. 4 Pre-exponential factors (upper plot; α_i) and steady-state emission intensity (lower plot; I) for Δ-[Ru(phen)$_2$dppz]$^{2+}$ bound to [poly(dA-dT)]$_2$ as a function of added NaCl. Upper Plot: [Nu]/[Ru] = 50; α_L (811 ns, ●); α_S (138 ns, ■). [Nu]/[Ru] = 6; α_L (863 ns, ○); α_S (176 ns, □). λ_{ex} = 440 nm; λ_{em} > 540 nm. Lower Plot: [Nu]/[Ru] = 50; measured intensity (▲); intensity predicted from lifetimes according to eqn (3) (◆). λ_{ex} = 440 nm; λ_{em} = 615 nm. [Ru] = 20 μM; 5 mM phosphate (pH 6.9); 25 °C.

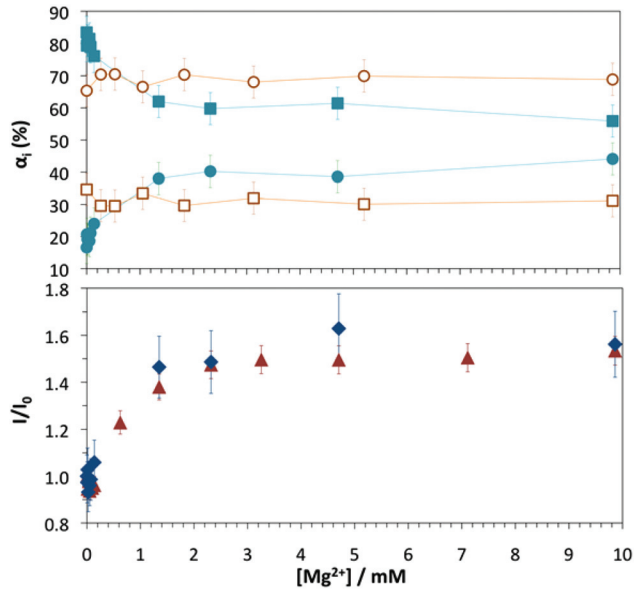

Fig. 5 Pre-exponential factors (upper plot; α_i) and steady-state emission intensity (lower plot; I) for Δ-[Ru(phen)$_2$dppz]$^{2+}$ bound to [poly(dA-dT)]$_2$ as a function of added $MgCl_2$. Upper Plot: [Nu]/[Ru] = 50; α_L (864 ns, ●); α_S (179 ns, ■). [Nu]/[Ru] = 6; α_L (745 ns, ○); α_S (126 ns, □). λ_{ex} = 440 nm; λ_{em} > 540 nm. Lower Plot: [Nu]/[Ru] = 50; measured intensity (▲); intensity predicted from lifetimes according to eqn (3) (◆). λ_{ex} = 440 nm; λ_{em} = 615 nm. [Ru] = 20 μM; 5 mM phosphate (pH 6.9); 25 °C.

calorimetry work in 150 mM NaCl[26] compared to our photophysics work in 5 mM phosphate.[18] The response to addition of $MgCl_2$ is similar, but the effects are observed at two orders of magnitude lower concentrations of added salt, *e.g.* only 2 mM Mg^{2+} is required for α_S to drop to ~60%. No displacement of [Ru(phen)$_2$dppz]$^{2+}$ is observed for [Mg^{2+}] ≤25 mM. In the crystal structures published to date,[29,30] the complexes are bound in isolated intercalation sites. This occurs despite tens of millimolar concentrations of spermine, Ba^{2+}, and cacodylate in the crystallization mixes which would be expected to favour canted dimers according to our model. However, the high density of material in the crystal and the observation that only certain sequences crystallize with Ru means that the crystal structures are snap-shots of particularly favourable potential binding geometries for those conditions rather than representations of thermodynamic minima in solution. Future photophysical experiments with the oligonucleotides used for crystallography, and on the crystals themselves are required to reveal more detail about binding at those particular binding sites.

At [Nu]/[Ru] = 6 (close to saturation of intercalation sites) in 5 mM phosphate, about 35% of the excited states decay with the short lifetime. Increasing ionic strength has only a small effect, with a drop to about 30% on addition of ≥150 mM NaCl or ≥2 mM $MgCl_2$, before displacement occurs. Our observation of much stronger effects of $MgCl_2$ is consistent with previous reports that Mg^{2+} ions bind to DNA at least 20 times higher than Na^+.[36–38]

Influence of temperature on emission

Temperature below the duplex melting transition (T_m ~ 70 °C) influences the lifetimes and pre-exponential factors of [Ru(phen)$_2$dppz]$^{2+}$ bound to [poly(dA-dT)]$_2$ (Table 1).

The variation of pre-exponential factors suggests a temperature-induced shift in equilibrium between different binding geometries, implying that dye–dye and dye–DNA interactions respond differently to temperature. For both enantiomers, the proportion of long-lived excited states increases with temperature, indicating a higher population of canted complexes. Thermodynamic analysis[26] of Δ-[Ru(phen)$_2$dppz]$^{2+}$ intercalation with [poly(dA-dT)]$_2$ indicates that interaction between symmetric (τ_S) and canted (τ_L) complexes is more exothermic (cooperative) than interaction between two oppositely canted complexes. Increasing temperature should thus favour the latter interaction, leading to an increase in the proportion of the long lifetime, as observed.

Table 1 Effect of temperature on the emission lifetimes of Δ- and Λ-[Ru(phen)$_2$dppz]$^{2+}$ with [poly(dA-dT)]$_2$. [Nu]/[Ru] = 50; [Ru] = 5 μM; 5 mM phosphate (pH 6.9); λ_{ex} = 440 nm; λ_{em} > 540 nm

	Δ-[Ru(phen)$_2$dppz]$^{2+}$				Λ-[Ru(phen)$_2$dppz]$^{2+}$			
T/°C	τ_L/ns	α_L/%	τ_S/ns	α_S/%	τ_L/ns	α_L/%	τ_S/ns	α_S/%
13	1100	*22*	99	*78*	562	*10*	42	*90*
22	776	*26*	135	*74*	382	*13*	38	*87*
33	771	*50*	148	*50*	349	*20*	37	*80*
45	804	*54*	181	*46*	329	*24*	46	*76*
54	787	*65*	202	*35*	282	*32*	48	*68*
64	738	*71*	178	*29*	218	*38*	45	*62*

Additionally, lifetime changes occur with increasing temperature, suggesting that increased dynamics in the DNA duplex in the pre-melting region leads to altered exposure of the intercalated dppz ligand to water. Lifetime reductions were also observed with $[poly(dG\text{-}dC)]_2$ (ESI;† Table S7), although the pre-exponential factors with that polynucleotide were relatively invariant.

Influence of nucleic acid sequence on emission

Fig. 6 and 7 show comparative emission intensities for Δ-$[Ru(phen)_2dppz]^{2+}$ with various DNA repeat sequences. Since $[Ru(phen)_2dppz]^{2+}$ does not emit in aqueous solution, the titration is carried out by adding the complex to a solution of polynucleotide. As the complex binds, the emission increases until the binding sites are saturated; thereafter, the emission plateaus, and the cutoff approximates the binding site size. With certain nucleic acids, *e.g.* $[poly(dA\text{-}dT)]_2$, the emission drops before saturation of intercalation sites (Fig. 6), due to quenching of intercalated complexes by externally associated molecules, as reported for lifetimes at [Nu]/[Ru] < 4.[17,18] However, this is not observed in higher salt buffer where external binding is minimized (ESI;† Fig. S1), and the binding site size is then confirmed to be 4–5 bases/complex as observed with other DNA sequences. Fig. 6 shows that Δ-$[Ru(phen)_2dppz]^{2+}$ emits more strongly with AT-rich than with GC-polynucleotides, which directly reflects the lifetimes observed with these nucleic acids.[17,18] The emission intensity for CT-DNA is intermediate between the two alternating polynucleotides.

We examined the emission of Δ-$[Ru(phen)_2dppz]^{2+}$ with mixed-sequence polynucleotides [poly(dA-dC)]·[poly(dG-dT)] and poly(dA-dG)]·[poly(dC-dT)] which contain the other base pair steps, as well as natural DNAs of random sequence having different GC : AT ratios. The relative emission quantum yields with these nucleic acids at a low binding ratio, compared to $[poly(dA\text{-}dT)]_2$, are presented in Fig. 7 (ESI;† Table S8). Clearly, there is a correlation between higher AT-content and increased emission, although there is deviation for some points. For example, the three polymers with 50% AT have different relative emissions (0.38–0.69), as do those with 100% AT (1.00–1.47). Thus, in addition to base pair composition, sequence context and conformation play a role in modulating the light switch effect.

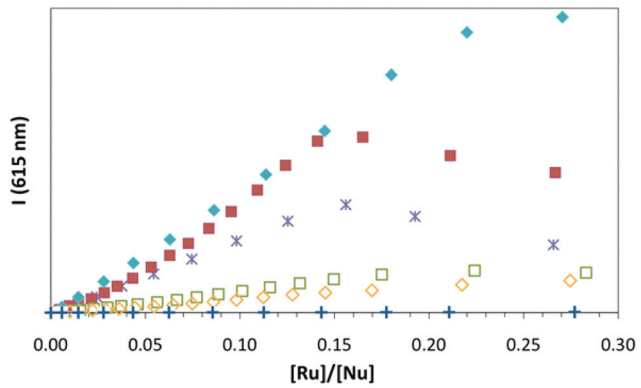

Fig. 6 Intensity titrations of Δ-$[Ru(phen)_2dppz]^{2+}$ with alternating and non-alternating duplex homo-polynucleotides compared to mixed sequence CT-DNA. $[Ru(phen)_2dppz]^{2+}$ is titrated into a solution of nucleic acid. [Nu] = 10 μM; 5 mM phosphate (pH 6.9); 25 °C; λ_{ex} = 440 nm; λ_{em} = 615 nm. CT-DNA (✳); $[poly(dA\text{-}dT)]_2$ (■); $[poly(dG\text{-}dC)]_2$ (□); [poly(dA)]·[poly(dT)] (◆); [poly(dG)]·[poly(dC)] (◇); no added DNA (+).

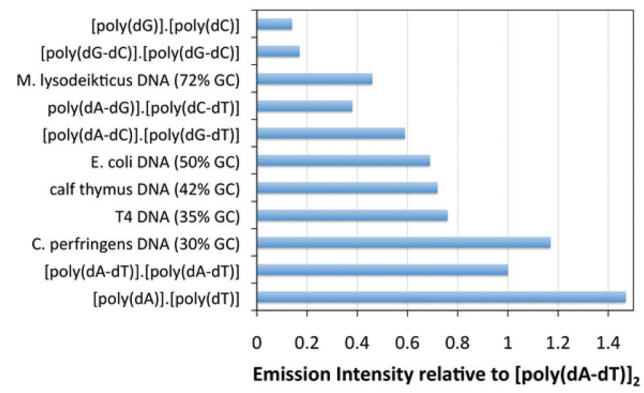

Fig. 7 Emission intensity of Δ-$[Ru(phen)_2dppz]^{2+}$ with various nucleic acids at low binding ratio, relative to that with $[poly(dA\text{-}dT)]_2$. [Ru] = 20 μM; [Nu]/[Ru] = 50; 5 mM phosphate (pH 6.9); 25 °C; λ_{ex} = 440 nm; λ_{em} = 615 nm.

Influence of nucleic acid conformation on emission

Fig. 8 compares the emission of Δ-$[Ru(phen)_2dppz]^{2+}$ with a variety of AT-rich DNA and RNA polynucleotides. In 5 mM phosphate, electrostatic interactions between the ruthenium complex and the polynucleotides are maximized, ensuring strong binding even to single-strands lacking classical intercalation sites.

We have previously used flow linear dichroism to demonstrate that Δ-$[Ru(phen)_2dppz]^{2+}$ intercalates with triplex [poly(dT)]*[poly(dA)]·[poly(dT)] as well as duplex [poly(dA)]·[poly-

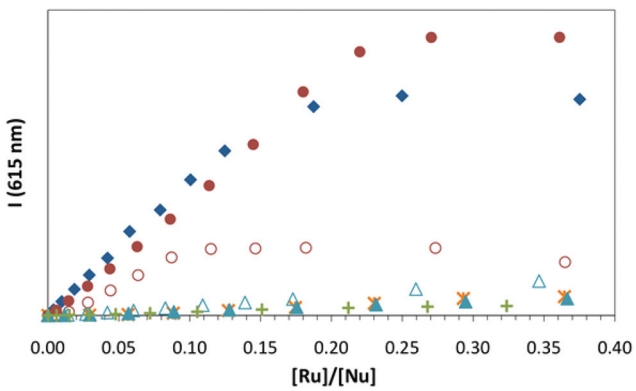

Fig. 8 Intensity titrations of Δ-$[Ru(phen)_2dppz]^{2+}$ with single- and triple-stranded polyribonucleotides and polydeoxyribonucleotides, compared to [poly(dA)]·[poly(dT)]. $[Ru(phen)_2dppz]^{2+}$ is titrated into a solution of nucleic acid. ss[Nu] = 5 μM; ds[Nu] = 10 μM; ts[Nu] = 15 μM; [PSS] = 5 μM; 5 mM phosphate (pH 6.9); 25 °C; λ_{ex} = 440 nm; λ_{em} = 615 nm. [poly(dA)]·[poly(dT)] (●); [poly(dT)]*[poly(dA)]·[poly(dT)] (◆); [poly(rA)]·[poly(rU)] (○); poly(dA) (▲); poly(rA) (△); poly(dT) (✳); PSS (+).

(dT)], and that it stabilizes the third strand much more than $[Ru(phen)_3]^{2+}$ or $[Ru(phen)_2bdppz]^{2+}$.[22] Fig. 8 shows that saturation of binding sites by Δ-$[Ru(phen)_2dppz]^{2+}$ occurs at [Nu]/[Ru] = 4.3 with duplex and [Nu]/[Ru] = 6.7 with triplex, consistent with intercalation between nearest neighbour base pairs and base triplets, respectively. On binding to triplex, 92% of the Δ-$[Ru(phen)_2dppz]^{2+}$ excited states decay with the long lifetime compared to 59% with duplex; τ_L is slightly shorter in triplex, but τ_S almost double.[17] Strong binding, long lifetimes and enhanced emission with triplex is consistent with intercalation from the Watson–Crick minor groove, resulting in improved protection of phenazine nitrogens from water. For both symmetric and canted intercalation models (ESI,† Fig. S3), the phenazine nitrogens are well protected in triplex and the terminal dppz ring stacks with the bases of the third strand. Emission with [poly(dA)]·[poly(dT)] and triplex is significantly higher than with $[poly(dA\text{-}dT)]_2$, suggesting that these more rigid DNA structures with narrow minor grooves and long persistence lengths provide optimal environments for enhanced emission.

Δ-$[Ru(phen)_2dppz]^{2+}$ shows moderate emission enhancement with [poly(rA)]·[poly(rU)], a duplex RNA, consistent with previous reports on racemic complexes.[1,16] Emission plateaus at [Nu]/[Ru] = 10, indicating that the complex has a large intrinsic binding site and/or that the binding constant is low so that binding sites are not saturated. Lifetimes are shorter with [poly(rA)]·[poly(rU)] than with [poly(dA)]·[poly(dT)][17] but, additionally, the observed emission is only 40% of that predicted from time-resolved data, implying that a substantial population of complex is not bound or is in a non-emissive environment. Our data point towards weak and possibly non-intercalative binding with RNA; unfortunately, the short chain length of our polynucleotide precludes linear dichroism analysis of binding geometry. This contrasts with a recent report that a related light-switch complex, $[Ru(phen)_2mdpz]^{2+}$, intercalates strongly with [poly(rA)]·[poly(rU)] and [poly(rU)]·[poly(rA)]*[poly(rU)].[23] However, we note that the dimeric complex $[(bpy)_2Ru(tpphz)Ru(bpy)_2]^{4+}$ emits with DNA even though intercalation does not occur.[39] Thus, we suggest that $[Ru(phen)_2dppz]^{2+}$ is groove bound to A-form RNA duplex, with emission enhancement arising from reduced accessibility of water to the phenazine nitrogens of the dppz ligand.

We observe weak enhancement of Δ-$[Ru(phen)_2dppz]^{2+}$ emission on interaction with the single-stranded polynucleotides poly(dA), poly(dT) and poly(rA) (Fig. 8), but no enhancement was observed in the presence of any mononucleotide. The quantum yields in all cases were too low for determination of lifetimes using frequency modulation. However, lifetimes from photon counting have been reported previously with single-stranded DNA.[19,20] In the former study, a threshold of 6 bases/oligonucleotide was required to induce emission of the racemate, suggesting that the polynucleotides form cavities for binding of $[Ru(phen)_2dppz]^{2+}$ which limit water accessibility.[19] In the latter study, tri-exponential decays were found for the enantiomers with poly(dA) and poly(dT) and, in contrast to the photophysics with duplexes, there was little dependence of lifetimes or pre-exponential factors on the nature of the bases or the enantiomer. This suggests that enhancement is not primarily due to stacking of the dppz ligand with bases in single strands, since poly(dA) would provide better overlap than poly(dT). We observe similarly low levels of emission enhancement when Δ-$[Ru(phen)_2dppz]^{2+}$ interacts with the hydrophobic polyanion polystyrenesulfonate (PSS). With this polyelectrolyte, stacking of dppz between adjacent phenyl residues is unlikely and enhanced emission probably arises from reduced water activity in the hydrophobic polyelectrolyte microenvironment, as also observed for $[Ru(phen)_3]^{2+}$.[40] Thus, it appears that intercalation, or aromatic stacking, is not a prerequisite for the observation of weak $[Ru(phen)_2dppz]^{2+}$ emission, but intercalation is necessary to produce strong emission enhancement.

Influence of major groove base modifications on emission

$[Ru(phen)_2dppz]^{2+}$ emission was investigated with natural DNA molecules containing bases modified with substituents in the major groove (Tables 2 and 3). Emission with T2- (33% GC) and T4-DNA (35% GC) was compared with CT-DNA (42% GC). The cytosine bases in the DNA of T-even bacteriophages are 5-hydroxymethylated in the major groove (to give 5-hydroxymethyl cytosine, HMC) and in T4-DNA, all HMC residues are further glycosylated. In T2-DNA, up to 75% of HMC bases are glycosylated. Furthermore, in both T2- and T4-DNA, 0.5–1.5% of adenine bases are methylated at N6 in the major groove. The 5-position on cytosine lies to one side of the major groove and even bulky substituents such as glucose can be accommodated without significantly altering the B-form structure of

Table 2 Time-resolved emission of Δ- and Λ-$[Ru(phen)_2dppz]^{2+}$ with natural nucleic acids at low binding density. [Ru] = 20 μM; [Nu]/[Ru] = 50; 5 mM phosphate (pH 6.9); 25 °C; λ_{ex} = 440 nm; λ_{em} > 540 nm

	Δ-$[Ru(phen)_2dppz]^{2+}$				Λ-$[Ru(phen)_2dppz]^{2+}$			
DNA	τ_L/ns	α_L/%	τ_S/ns	α_S/%	τ_L/ns	α_L/%	τ_S/ns	α_S/%
AT_2	737	*26*	135	*74*	327	*10*	36	*90*
CT	794	*26*	134	*74*	262	*6*	37	*94*
T2	783	*21*	108	*79*	298	*4*	34	*96*
T4	856	*23*	123	*77*	244	*7*	36	*93*
GC_2	248	*78*	67	*22*	165	*4*	41	*96*

AT_2 = $[poly(dA\text{-}dT)]_2$; GC_2 = $[poly(dG\text{-}dC)]_2$.

Table 3 Time-resolved emission of Δ- and Λ-$[Ru(phen)_2dppz]^{2+}$ with natural nucleic acids at high binding density. [Ru] = 20 μM; [Nu]/[Ru] = 2; 5 mM phosphate (pH 6.9); 25 °C; λ_{ex} = 440 nm; λ_{em} > 540 nm

	Δ-$[Ru(phen)_2dppz]^{2+}$				Λ-$[Ru(phen)_2dppz]^{2+}$			
DNA	τ_L/ns	α_L/%	τ_S/ns	α_S/%	τ_L/ns	α_L/%	τ_S/ns	α_S/%
AT_2	464	*57*	68	*43*	243	*47*	53	*53*
CT	753	*47*	181	*53*	544	*25*	103	*75*
T4	869	*46*	225	*54*	527	*29*	101	*31*
GC_2	174	*35*	54	*65*	116	*29*	37	*71*

AT_2 = $[poly(dA\text{-}dT)]_2$; GC_2 = $[poly(dG\text{-}dC)]_2$.

DNA. However, these substituents are know to alter the extent of DNA hydration in the major groove.[41]

Table 2 indicates that Δ-[Ru(phen)$_2$dppz]$^{2+}$ selects for alternating (dA-dT)$_n$ intercalation sites in random DNA sequences at low binding ratio. At [Nu]/[Ru] = 50 there is a large excess of binding sites per complex, and the lifetimes and pre-exponential factors with CT-DNA are very similar to those with [poly(dA-dT)]$_2$. The lifetimes and pre-exponential factors for the Λ-enantiomer are intermediate between those with [poly(dA-dT)]$_2$ and [poly(dG-dC)]$_2$. Thus, Λ-[Ru(phen)$_2$dppz]$^{2+}$ has mixed sequence preference in natural DNA. Hydroxymethylation and glycosylation of cytosine in the major groove do not substantially affect the photophysics of either enantiomer at [Nu]/[Ru] = 50, apart from increasing τ_L consistent with increased protection from groove-localized water when DNA has a bulky DNA major-groove substituent. Of course, if [Ru(phen)$_2$dppz]$^{2+}$ is predominantly bound in AT-rich regions, these major groove substituents in GC-rich regions would not be expected to greatly affect the binding or photophysics of the complex. However, as the binding ratio increases so that the complex must also occupy GC sites, the effect of the substituents should become more pronounced if [Ru(phen)$_2$dppz]$^{2+}$ resides in the major groove.

At [Nu]/[Ru] = 2, where intercalation sites are saturated, the photophysics with mixed-sequence DNAs are different from those with either alternating polynucleotide (Table 3). All lifetimes are longer, indicating substantially improved protection from water when the complexes are bound in close proximity. For either enantiomer, there is a marked similarity of the photophysics with CT- and T4-DNA under these conditions, indicating that glycosylation in the major groove does not significantly affect the binding of [Ru(phen)$_2$dppz]$^{2+}$ to DNA, even when they are closely intercalated. Both τ_L and τ_S for Δ-[Ru(phen)$_2$dppz]$^{2+}$ are longer with T4-DNA, implying better protection from water, but there is little difference for Λ-[Ru(phen)$_2$dppz]$^{2+}$ which is also reflected in the steady-state emission intensities (ESI;† Fig. S2). These observations are consistent with intercalation of [Ru(phen)$_2$dppz]$^{2+}$ from the minor groove in solution and with glycosylation altering major groove hydration[41] thus reducing its accessibility to phenazine nitrogens of the intercalated dppz ligand.

Discussion

Intercalative geometry dictates photophysical response

When [Ru(phen)$_2$dppz]$^{2+}$ is bound to nucleic acids, emission decay is typically biexponential. We have recently proposed a binding model for [Ru(phen)$_2$dppz]$^{2+}$ bound to [poly(dA-dT)]$_2$ in which the complex has two intercalation geometries, where their relative populations are dictated by a balance of cooperative and anti-cooperative complex–complex interactions and complex–DNA interactions.[26] The two lifetimes reflect differential exposure of the phenazine nitrogens to water for the two geometries. The short lifetime is assigned to symmetric, head-on intercalation of the dppz ligand and occurs for isolated molecules and within contiguous sequences. The long lifetime is assigned to canted insertion of the dppz ligand and this geometry occurs at either end of contiguous sequences. In the absence of cooperative interactions, isolated symmetric complexes with short lifetimes are expected to dominate at high [Nu]/[Ru] values and this is observed for Λ-[Ru(bpy)$_2$dppz]$^{2+}$ with [poly(dA-dT)]$_2$. However, for Δ-[Ru(phen)$_2$dppz]$^{2+}$ with [poly(dA-dT)]$_2$, canted duplets occur even at low binding ratios due to high cooperativity for such a configuration[26] arising from a favourable interactions between phenanthroline and the DNA backbone and possibly associated with an allosteric conformational change. By contrast, when bipyridine is the ancillary ligand, canted duplets are anti-cooperative, and there is no favourable counterbalancing ligand-backbone interaction.

The recent crystal structure of Λ-[Ru(phen)$_2$dppz]$^{2+}$ bound to a decamer led to the observation that the base pairs (GG/CC) around a canted complex have a twist of ~25° and those around a symmetric complex (TA/TA) have a twist of ~40°.[30] When the central TA/TA base pair was changed to AT/AT, no intercalation was observed at this site,[30] although symmetric intercalation of Δ-[Ru(bpy)$_2$dppz]$^{2+}$ was observed at an AT/AT site in a mismatched oligonucleotide where the bpy ligands stacked with flipped out adenines in the minor groove.[25] We surmise that the ability of base pair steps to adopt different twisting angles around an intercalated complex is an important factor in dictating the orientation of the complex, and the allosteric change we propose for canting might be related to this ability. Thus, the conformational adaptability and the flexibility of the DNA molecule, coupled with the nature of the complex, plays a critical role in modulating the relative populations of different intercalation geometries.

DNA and binding response to increasing ionic strength

For [Ru(phen)$_2$dppz]$^{2+}$/[poly(dA-dT)]$_2$ at high [Nu]/[Ru] ratios, the long lifetime amplitude increases substantially with increasing ionic strength, implying a shift in equilibrium from isolated symmetrically intercalated complexes toward canted duplets. DNA has two overarching responses to changes in ionic strength. First, the thermal denaturation temperature (T_m) for breaking base pair H-bonds and melting to single strands increases with increasing salt as inter- and intra-strand electrostatic repulsion is diminished. Frank-Kaminetskii and coworkers have shown that this is due to variation of the base-stacking free energy change (ΔG_{st}), since the free energy change for base-pairing (ΔG_{HB}) does not change with ionic strength.[42] Second, as a consequence of attenuated electrostatic repulsion, the persistence length of DNA drops with increasing salt,[43–45] indicating increased macroscopic flexibility and susceptibility to elastic deformation.

We hypothesise that the greater flexibility at higher ionic strength make DNA more amenable to allosteric changes that enhance cooperative complex–DNA interactions compared to anti-cooperative complex–complex interactions. This would produce the experimentally observed higher population of long-lived canted duplets.

DNA and binding response to increasing temperature

With increasing temperature, the population of complexes with a long emission lifetime increases for both enantiomers with $[poly(dA\text{-}dT)]_2$, implying a shift from symmetric to canted intercalation, as observed also with increasing ionic strength. The long emission lifetime (τ_L) is more sensitive to temperature than it is to salt, in particular decreasing markedly between 13 and 22 °C for both enantiomers, although τ_S is relatively invariant. A decrease in τ_L could reflect either a change in conformation of the intercalation site that makes the dppz nitrogens more accessible to water at high temperature, or a change in the dynamics of the major groove hydration layer, but these cannot be distinguished without structural studies. An intriguing possibility is that the complex could reside in the major groove at low temperatures, since the nmr experiment that indicates such binding for Δ-$[Ru(phen)_2dppz]^{2+}$ was carried out at a low temperature of 7 °C,[46] whereas the nmr experiment that places the Δ-$[Ru(Me_2phen)_2dppz]^{2+}$ in the minor groove was carried out at 45 °C.[27] To interpret changes in pre-exponential factors, we consider the effect of temperature on the conformational variability of DNA. Rising temperature destabilizes the DNA duplex until thermal denaturation and separation of strands occurs at T_m, as a result of a decrease in stacking free energy.[42] Premelting transitions occur in the 5–60 °C range, where the DNA becomes more flexible and its persistence length decreases dramatically as base pair "breathing" occurs.[47,48] This can be related to the proposal that transient sharp bends occur in sub-persistence length DNA even at room temperature, possibly at regions of base pair breathing.[49–51] This behaviour is not accounted for by the wormlike chain model for DNA but, clearly, is a significant phenomenon that become increasingly important at high temperatures.[48] An increase in DNA flexibility with temperature is similar to that observed with increasing ionic strength. Indeed, in both cases we observe a tendency towards a higher population of canted duplets as cooperative complex–DNA interactions become favoured. Since temperature and ionic strength have opposite effects on stacking free energy,[42] differences in base pair stacking are unlikely to be the main driver for the observed effects. Thus DNA flexibility and deformability must be key in controlling these observed phenomena. Recently, the binding of a Ru-dppz complex has been shown to change from intercalative at low temperature to groove binding at room temperature and above, illustrating how temperature dramatically influences dye–DNA interactions.[52]

Sequence-dependent conformational plasticity of DNA

A further point of interest is the difference in the temperature-dependent behaviour of $[Ru(phen)_2dppz]^{2+}$ when bound to $[poly(dA\text{-}dT)]_2$ or $[poly(dG\text{-}dC)]_2$. These alternating polynucleotides have similar pseudo-B-form secondary structures consisting of dinucleotide repeat units.[53–56] For both enantiomers with $[poly(dG\text{-}dC)]_2$, there is very little variation of pre-exponential factor with increasing temperature, implying that the populations of the canted and symmetrically oriented complexes do not change, although lifetimes change as they do with $[poly(dA\text{-}dT)]_2$. From analysis of crystal structures of oligonucleotides and DNA–protein complexes, the conformational plasticity at the base pair dimer and tetramer level is reported to be much greater, and the minor groove significantly wider, for GC- than AT-rich steps.[57–60] Moreover, it is reported that inflexible T-A steps can act as hinges in protein–DNA structures[57] and between DNA A-tracts by widening the minor groove,[59] although they are also deformable enough to be accommodated in a narrow groove.[59]

On the basis of these observations, we propose that $[poly(dG\text{-}dC)]_2$ is sufficiently flexible at low temperature to adopt the conformation required to accommodate canted dimers of Δ-$[Ru(phen)_2dppz]^{2+}$, whereas $[poly(dA\text{-}dT)]_2$ needs some input of energy to achieve this. It has been reported that $[poly(dA\text{-}dT)]_2$ switches between two distinct conformations in solution as temperature is raised in the pre-melting region at low ionic strength.[61,62] It is likely that this conformational switch is related to the observed changes in $[Ru(phen)_2dppz]^{2+}$ photophysics at high [Nu]/[Ru] which we ascribe to a change in binding geometry.

However care must be exercised with crystal structure analyses since it has been suggested that these may overestimate the rigidity of base-pair steps, making deformable steps appear as the most rigid, *e.g.* AA, TA and AT.[63] Indeed, a recent study of sequence effects indicates that the persistence length of GC-rich DNA is greater than AT-rich DNA;[64] from those results, the persistence lengths of the two polynucleotides are predicted to be 42.8 nm for $[poly(dA\text{-}dT)]_2$ and 50.3 nm $[poly(dG\text{-}dC)]_2$. On the other hand, the average persistence length of short random sequence DNA is reported to be relatively sequence-insensitive.[65] Contradictory conclusions about the sequence dependence of persistence length and DNA flexibility have long been debated,[43] and this area remains unclear. Recent work suggests that use of linear dichroism has good potential for understanding the effects of ionic strength and temperature on the flexibility of different DNA sequences, and should help to understand these phenomena better in future.[66] At present, predicting the ability of DNA to adapt to small molecule binding, and correlating the conformational deformability of base-pair steps with large scale sequence specific conformational plasticity is not straightforward. Nevertheless, we consider that DNA conformational adaptability plays a critical role in determining binding geometries. We look forward to the emergence of more structural information about the binding of $[Ru(L)_2dppz]^{2+}$ in different sequences and secondary structures, to facilitate better understanding of the interactions that are critical in determining binding geometry.

Conclusions

This work demonstrates how the emission of $[Ru(phen)_2dppz]^{2+}$ bound to nucleic acids depends on ionic

strength, temperature, and the nature of the nucleic acid, but not significantly on bulky substituents in the major groove. These findings complement our previous findings that the emission depends on enantiomer, ancillary ligand, and DNA sequence,[17,18,26] and reveals further complexity inherent in DNA recognition by metal complexes. The photophysics of $[Ru(phen)_2dppz]^{2+}$ bound to nucleic acids are extraordinarily sensitive to the exposure of the uncoordinated dppz nitrogens to groove-localized water, making this complex an exceptionally sensitive reporter of subtle changes in binding geometry. We have attributed the two lifetimes observed for intercalated $[Ru(phen)_2dppz]^{2+}$ with canted and symmetric intercalation, and made assignments based on comparison with the recent crystal structure.[30] Thus, in $[poly(dA\text{-}dT)]_2$, symmetric intercalation with both nitrogens are exposed to the hydrated major groove is associated with the short lifetime. The relative amplitudes of long and short lifetimes reflect the proportion of complex bound with each intercalation geometry. These amplitudes are markedly affected by ionic strength and by temperature, likely as a result of changes in the flexibility and conformational plasticity of DNA when these conditions are varied. Increasing ionic strength attenuates inter- and intrastand DNA electrostatic repulsion which reduces rigidity, and a rise in temperature allows increased conformational freedom. Additionally, the lifetimes and amplitudes both depend strongly on DNA sequence and conformation, as well as on the stereochemistry of the complex. Sensitivity to so many parameters makes it difficult to interpret photophysical changes when mixed sequences, unusual sequences, or racemic mixtures are used. However, for highly defined nucleic acid systems with a single enantiomer, the luminescence of $[Ru(phen)_2dppz]^{2+}$ can provide a useful readout that is amenable to structural interpretation, but only if time-resolved data is examined alongside steady-state emission.

Acknowledgements

EMT gratefully acknowledges the EU Marie Curie Fellowship programme and EPSRC (GR/S23315/01) for financial support. AWMcK acknowledges receipt of an EPSRC DTA studentship from Newcastle University School of Chemistry. PL acknowledges funding from The Swedish Research Council (VR). EMT and PL are grateful to COST D35 for networking and collaborative opportunities.

References

1 A. E. Friedman, J.-C. Chambron, J.-P. Sauvage, N. J. Turro and J. K. Barton, *J. Am. Chem. Soc.*, 1990, **112**, 4960–4962.
2 C. Hiort, P. Lincoln and B. Nordén, *J. Am. Chem. Soc.*, 1993, **115**, 3448–3454.
3 E. Amouyal, A. Homsi, J.-C. Chambron and J.-P. Sauvage, *J. Chem. Soc., Dalton Trans.*, 1990, 1841–1845.
4 R. B. Nair, B. M. Callum and C. J. Murphy, *Inorg. Chem.*, 1997, **36**, 962–965.
5 J.-C. Chambron and J.-P. Sauvage, *Chem. Phys. Lett.*, 1991, **182**, 603–607.
6 X.-Q. Guo, F. N. Castellano, L. Li and J. R. Lakowicz, *Biophys. Chem.*, 1998, **71**, 51–62.
7 E. J. C. Olson, D. Hu, A. Hormann, A. M. Jonkman, M. R. Arkin, E. D. A. Stemp, J. K. Barton and P. F. Barbara, *J. Am. Chem. Soc.*, 1997, **119**, 11458–11467.
8 B. Önfelt, P. Lincoln, B. Nordén, J. S. Baskin and A. H. Zewail, *Proc. Natl. Acad. Sci. U. S. A.*, 2000, **97**, 5708–5713.
9 C. Coates, J. Olofsson, M. Coletti, J. J. McGarvey, B. Önfelt, P. Lincoln, B. Nordén, E. M. Tuite, P. Matousek and A. W. Parker, *J. Phys. Chem. B*, 2001, **105**, 12653–12664.
10 J. Olofsson, B. Önfelt, P. Lincoln, B. Nordén, P. Matousek, A. W. Parker and E. Tuite, *J. Inorg. Biochem.*, 2002, **91**, 286–297.
11 A. W. McKinley, P. Lincoln and E. M. Tuite, *Coord. Chem. Rev.*, 2011, **255**, 2676–2692.
12 M. K. Brennaman, J. H. Alstrum-Acevedo, C. N. Fleming, P. Jang, T. J. Meyer and J. M. Papanikolas, *J. Am. Chem. Soc.*, 2002, **124**, 15094–15098.
13 M. K. Brennaman, T. J. Meyer and J. M. Papanikolas, *J. Phys. Chem. A*, 2004, **108**, 9938–9944.
14 B. Önfelt, J. Olofsson, P. Lincoln and B. Nordén, *J. Phys. Chem. A*, 2003, **107**, 1000–1009.
15 J. Olofsson, B. Önfelt and P. Lincoln, *J. Phys. Chem. A*, 2004, **108**, 4391–4398.
16 Y. Jenkins, A. E. Friedman, N. J. Turro and J. K. Barton, *Biochemistry*, 1992, **31**, 10809–10816.
17 E. Tuite, P. Lincoln and B. Nordén, *J. Am. Chem. Soc.*, 1997, **119**, 239–240.
18 A. W. McKinley, J. Andersson, P. Lincoln and E. M. Tuite, *Chem.–Eur J.*, 2012, **18**, 15142–15150.
19 C. G. Coates, J. J. McGarvey, P. L. Callaghan, M. Coletti and J. G. Hamilton, *J. Phys. Chem. B*, 2001, **105**, 730–735.
20 J. M. Kim, J.-M. Lee, J. Y. Choi, H. M. Lee and S. K. Kim, *J. Inorg. Biochem.*, 2007, **101**, 1386–1393.
21 S. Shi, X. Geng, J. Zhao, T. Yao, C. Wang, D. Yang, L. Zheng and L. Ji, *Biochimie*, 2010, **92**, 370–377.
22 S.-D. Choi, M.-S. Kim, S. K. Kim, P. Lincoln, E. Tuite and B. Nordén, *Biochemistry*, 1997, **36**, 214–223.
23 L.-F. Tan, J. Liu, J.-L. Shen, X.-H. Liu, L.-L. Zeng and L.-H. Jin, *Inorg. Chem.*, 2012, **51**, 4417–4419.
24 M. H. Lim, H. Song, E. D. Olmon, E. E. Dervan and J. K. Barton, *Inorg. Chem.*, 2009, **48**, 5392–5397.
25 H. Song, J. T. Kaiser and J. K. Barton, *Nat. Chem.*, 2012, **4**, 615–620.
26 J. Andersson, L. Fornander, M. Abrahamsson, E. M. Tuite, P. Nordell and P. Lincoln, *Inorg. Chem.*, 2013, **52**, 1151–1159.
27 A. Greguric, I. D. Greguric, T. W. Hambley, J. R. Aldrich-Wright and J. C. Collins, *J. Chem. Soc., Dalton Trans.*, 2002, 849–855.
28 P. Waywell, V. Gonzalez, M. R. Gill, H. Adams, A. J. H. M. Meijer, M. P. Williamson and J. A. Thomas, *Chem.–Eur. J.*, 2010, **16**, 2407–2417.

29 J. P. Hall, K. O'Sullivan, A. Naseer, J. A. Smith, J. M. Kelly and C. J. Cardin, *Proc. Natl. Acad. Sci. U. S. A.*, 2011, **108**, 17610–17614.
30 H. Niyazi, J. P. Hall, K. O'Sullivan, G. Winter, T. Sorensen, J. M. Kelly and C. J. Cardin, *Nat. Chem.*, 2012, 621–628.
31 E. A. Lewis, M. Munde, S. Wang, M. Rettig, V. Le, V. Machha and W. D. Wilson, *Nucleic Acids Res.*, 2011, **39**, 9649–9658.
32 P. Lincoln and B. Nordén, *J. Phys. Chem. B*, 1998, **102**, 9583–9594.
33 E. Tuite and B. Nordén, *Bioorg. Med. Chem.*, 1995, **3**, 701–711.
34 *Principles of Fluorescence Spectroscopy*, ed. J. R. Lakowicz, 2nd edn, Springer, 1999.
35 I. Haq, P. Lincoln, D. Suh, B. Nordén, B. Z. Chowdhry and J. B. Chaires, *J. Am. Chem. Soc.*, 1995, **117**, 4788–4796.
36 Y. Bai, M. Greenfeld, K. J. Travers, V. B. Chu, J. Lipfert, S. Doniach and D. Herschlag, *J. Am. Chem. Soc.*, 2007, **129**, 14981–14988.
37 V. V. Rybenkov, A. V. Vologodskii and N. R. Cozzarelli, *Nucleic Acids Res.*, 1997, **25**, 1412–1418.
38 M. D. Paulsen, C. F. Anderson and M. T. J. Record, *Biopolymers*, 1988, **27**, 1249–1265.
39 D. A. Lutterman, A. Chouai, Y. Liu, Y. Sun, C. D. Stewart, K. R. Dunbar and C. Turro, *J. Am. Chem. Soc.*, 2008, **130**, 1163–1170.
40 E. M. Tuite, D. B. Rose, P. M. Ennis and J. M. Kelly, *Phys. Chem. Chem. Phys.*, 2012, **14**, 3681–3692.
41 R. A. J. Warren, *Annu. Rev. Microbiol.*, 1980, **34**, 137–158.
42 P. Yakovchuk, E. Protozanova and M. D. Frank-Kamenetskii, *Nucleic Acids Res.*, 2006, **34**, 564–574.
43 P. J. Hagerman, *Ann. Rev. Biophys. Biophys. Chem.*, 1988, **17**, 265–286.
44 C. G. Baumann, S. B. Smith, V. A. Bloomfield and C. Bustamante, *Proc. Natl. Acad. Sci. U. S. A.*, 1997, **94**, 6185–6190.
45 A. Savelyev, *Phys. Chem. Chem. Phys.*, 2012, **14**, 2250–2254.
46 C. M. Dupureur and J. K. Barton, *J. Am. Chem. Soc.*, 1994, **116**, 10286–10287.
47 S. Geggier, A. Kotlyar and A. Vologodskii, *Nucleic Acids Res.*, 2011, **39**, 1419–1426.
48 N. Theodorakopoulos and M. Peyard, *Phys. Rev. Lett.*, 2012, **108**, 078104 (1–4).
49 T. E. Cloutier and J. Widom, *Proc. Natl. Acad. Sci. U. S. A.*, 2005, **102**, 3645–3650.
50 P. Wiggins, T. van der Heijden, F. Moreno-Herrero, A. Spakowitz, R. Phillips, J. Widom, C. Dekker and P. C. Nelson, *Nat. Nanotechnol.*, 2006, **1**, 137–141.
51 R. Vafabakhsh and T. Ha, *Science*, 2012, **337**, 1097–1101.
52 M. G. Walker, V. Gonzalez, E. Chekmeneva and J. A. Thomas, *Angew. Chem., Int. Ed.*, 2012, **124**, 12273–12276.
53 A. Klug, A. Jack, M. A. Viswamitra, O. Kennard, Z. Shakked and T. A. Steitz, *J. Mol. Biol.*, 1979, **131**, 669–680.
54 D. J. Patel, L. L. Canuel and F. M. Pohl, *Proc. Natl. Acad. Sci. U. S. A.*, 1979, **76**, 2508–2511.
55 R. Lavery, B. Pullman and S. Corbin, *Nucleic Acids Res.*, 1981, **9**, 6539–6552.
56 S. Arnott, R. Chandrasekaran, L. C. Puigjaner, J. K. Walker, I. H. Hall and D. L. Birdsall, *Nucleic Acids Res.*, 1983, **11**, 1457–1474.
57 W. Olson, A. Gorin, X. Lu, L. Hock and V. Zhurkin, *Proc. Natl. Acad. Sci. U. S. A.*, 1998, **95**, 11163–11168.
58 D. Svozil, J. Kalina, M. Omelka and B. Schneider, *Nucleic Acids Res.*, 2008, **36**, 3690–3706.
59 R. Rohs, A. M. West, A. Sosinsky, P. Liu, R. S. Mann and B. Honig, *Nature*, 2009, **461**, 1248–1254.
60 C. Ougey, N. Foloppe and B. Hartmann, *PLoS One*, 2010, **5**, e15931.
61 S. Brahms, J. Brahms and K. E. Van Holde, *Proc. Natl. Acad. Sci. U. S. A.*, 1976, **73**, 3453–3457.
62 J. Kypr, J. Sági, A. Szabolcs, K. Ebinger, L. Ötvös and M. Vorličková, *Gen. Physiol. Biophys.*, 1990, **9**, 415–418.
63 F. Pedone, F. Mazzei, M. Matzeu and F. Barone, *Biophys. Chem.*, 2001, **94**, 175–184.
64 S. Geggier and A. Vologodskii, *Proc. Natl. Acad. Sci. U. S. A.*, 2010, **107**, 15421–15426.
65 A. J. Mastroianni, D. A. Sivak, P. L. Geissler and A. P. Alivisatos, *Biophys. J.*, 2009, **97**, 1408–1417.
66 M. Rittman, S. V. Hoffmann, E. Gilroy, M. R. Hicks, B. Finenstadt and A. Rodger, *Phys. Chem. Chem. Phys.*, 2012, **14**, 353–366.

